Assessing Forest Degradation in Duhok Province, Iraq (2000–2024) Using Geospatial Techniques

Nofa Bahzad Mohammed Alsinayi 1, Mohammed Hadeat Obeyed Alzuhary 2 and Heman Abdulkhaleq A. Gaznayee 3* ,
1Department of Forestry, College of Agricultural Engineering Sciences, University of Duhok, Duhok, Kurdistan Region,Iraq; nofa.mohammed@uod.ac
2Department of Forestry, College of Agricultural Engineering Sciences, University of Duhok, Duhok, Kurdistan Region,Iraq;mohammed.obeyd@uod.ac
3Department of Forestry, College of Agriculture Engineering Science, Salahaddin University, Erbil, Kurdistan Region, Iraq; heman.ahmed@su.edu.krd; ORCID : https://orcid.org/0000-0002-1549-407X *Correspondence: heman.ahmed@su.edu.krd

Abstract :
Forest ecosystems in this region, particularly within Zakho, and Duhok districts, have experienced significant environmental stress due to persistent armed conflicts, fires, climate variability, and unsustainable land use. This study assesses forest degradation in Duhok Province, Iraq, from 2000 to 2024 by employing remote sensing and geospatial techniques. Utilizing satellite-derived spectral indices including Normalized Difference Vegetation Index (NDVI), Modified Soil Adjusted Vegetation Index (MSAVI2), Normalized Difference Moisture Index (NDMI), and LST, this analysis quantifies the extent and severity of vegetation loss, moisture reduction, and increased land surface temperatures (LST). Results indicate dramatic forest cover declines: Zakho's forested area decreased from 716.6 km² (49.3%) in 2000 to 521.8 km² (35.9%) by 2024. While Duhok forests decreased from 622.8 km² (61.4%) to 416.5 km² (41%). Moisture analysis (NDMI) in Zakho showed a sharp rise in dry areas from 340.9 km² (23.5%) to 507.7 km² (34.9%) and a reduction of moist zones. Land Surface Temperature (LST) increased dramatically, with extreme temperature zones (≥50°C) rising from 29 km² (2%) to 235.7 km² (16.2%), indicating intensified desertification and heat stress linked to vegetation loss. The analysis underscores significant ecological consequences driven by conflict-induced environmental degradation, unsustainable development, and climatic stress. This research emphasizes the critical need for targeted reforestation, robust environmental governance, sustainable land management, and continuous monitoring to achieve sustainable development goals (SDGs) related to climate action and terrestrial ecosystem conservation.

Keywords: Forest degradation, Remote sensing, Geospatial techniques, NDVI, NDMI, Duhok Province, and Iraq.

Introduction

For many years, climate change, characterized by global warming, has been a source of international worry[1]. Human-caused deforestation has been occurring for many centuries. Nevertheless, the quick and dramatic loss of forests and their degradation in recent decades, along with the significant environmental, social, and economic consequences, have drawn more global interest in measuring and monitoring areas covered by forests all around[2]. Land structures could experience slow changes over time (like urbanization or economic growth) or sudden shocks (such as socio-economic, environmental, and military conflicts)[3], [4]Among the most serious concerns that might affect a land structure are armed conflicts. Armed conflicts have many erratic effects on the environment [4]. They may, for instance, affect deforestation rates[5]. change land-use intensity and cause land abandonment [6]. Research showed, on the one hand, that conflict zones have seen reforestation and improved biodiversity preservation as a consequence of land abandonment [7.[

In many countries that are afflicted by or recovering from war, deforestation is a recurring issue that is often linked to a location-dependent confluence of insecurity-related issues. While deforestation may have short-term benefits, it may have long-term negative consequences on biodiversity, local livelihoods, weather, and habitability. Additional studies are being conducted to examine the impact that armed conflict plays in the incidence and spread of vegetation fires, with some findings revealing links between increasing conflict and fires[8]. Although there has been a recent increase in interest in the topic, research on the environmental effects of conflict remains complex and full of unknowns. The most significant of these is that conflict zones are often inaccessible to researchers due to security concerns, necessitating the remote collection of data .

In this context, geographic information systems (GIS) and remote sensing have proved useful, providing accurate spatial data on changes in land cover and the health of forests[9].For monitoring changes in land use, satellite remote sensing is essential, particularly in dangerous areas [10]. By using satellite remote sensing and geospatial analysis, changes in forest cover and their geopolitical contexts may be examined and measured. Monitoring of battling land ecosystems is becoming almost continual due to the increasing quantity of freely available Earth observation data with a pretty high geographical and/or temporal precision. Furthermore, by using extensive satellite data sets, including optical data from the Landsat archive, we may analyze military conflicts that go back to the 1980s [6]. Venema et al. (2005) assert that using remote sensing techniques and producing spatial representations, such maps, to pinpoint the precise locations and extent of deforestation is the only way to carry out effective forest monitoring and management[11]. These tools help academics and policymakers create focused interventions for forest conservation by providing crucial insights into how war, conflict, and climate change affect forest ecosystems[12.[

Numerous researches have examined the connection between forest cover and spectral indices including NDVI, NDMI, MSAVI2, and LST. These indices are often used as models for temperature, moisture, water content, and cover of vegetation, and their correlations with forest cover may provide crucial information on how changes in forest cover affect the ecosystem. The statistical association between forest cover and NDVI in the Indian Himalayan area was examined in one research by Singh et al.[13].The scientists estimated NDVI using remote sensing data and discovered a strong positive association between NDVI and forest cover, suggesting that NDVI may be a trustworthy measure of forest cover. The scientists estimated LST using remote sensing data and discovered a negative correlation between LST and forest cover, suggesting that forest cover may aid in lowering surface temperatures[14], [15]. The authors estimated NDMI using remote sensing data and discovered a strong positive association between NDMI and forest cover, suggesting that NDMI may be a trustworthy measure of forest cover[16], [17]. Hossain et al. (2020) investigated the connection between

ISSN 2072-3857

spectral indices and forest cover in Bangladesh's Sundarbans mangrove forest. The authors estimated NDVI, LST, NDMI, and TCW using remote sensing data[18]. They discovered strong positive correlations between these indices and forest cover, suggesting that they may be accurate predictors of forest cover. To sum up, spectral indices like LST, MSAVI2, NDVI, and NDMI may be employed as trustworthy measures of forest cover. Estimating these indicators and examining their statistical correlations with forest cover using remote sensing data might provide important information about the environmental effects of shifting forest cover. This study analyzes climate impact on forest degradation in Duhok using remote sensing and GIS. It explores governance, environmental degradation to promote UN's SDGs. Goal is to assess forest degradation in Duhok using satellite data and GIS. This supports sustainable land management and forest protection (SDG 15). Analyzing climate effect on forest loss through temperature and precipitation variations is another goal. Climate variability affects vegetation health, intensifying forest stress, wildfires, and drought (SDG 13 .(

Materials and Methods

Study Area

The research was conducted in Duhok Governorate (DU), encompassing Three districts: Amadiya, Duhok (Center), and Zakho, (Figure 1). DU's climate mirrors that of the Mediterranean, characterized by moderate to chilly and damp winters and warm to scorching and arid summers. The average yearly temperature ranges from 19.3°C to 21.2°C, with winter temperatures spanning from 0°C to 15°C and summer temperatures from 20°C to 37°C (Figure 2) [19], [20]. The annual rainfall averages between 500 and 1,000 millimeters. Forest encompass 28.4% of the region, with the majority of farmlands located near villages (Nations, 2010.(

Methodology

The methodology initiated in Figure 3, commencing with data acquisition, involves satellite imagery from Landsat 5 Thematic Mapper (TM), Landsat 7 Enhanced Thematic Mapper Plus (ETM+), Landsat 8 Operational Land Imager (OLI), and Sentinel 1 & 2, in conjunction with field measurements obtained through Google Earth. Thermal Infrared Sensor (TIRS) data is also harnessed for thermal infrared processing. These datasets serve as the fundamental inputs for subsequent analysis[23], [24], [25]. The satellite imagery goes through several procedures during the data preparation stage, such as image resampling and atmospheric corrections to determine bottom-of-atmosphere (BOA) reflectance. To improve spatial resolution, pan-sharpening is used for Landsat data [23]. After defining the boundaries of the study area, the area of interest is highlighted using mosaicking and sub-setting. By analyzing large data sets and seeing patterns and trends, machine learning algorithms can recognize changes in the forest cover. These detection processes have become much more accurate and efficient due to the combination of machine learning and remote sensing data. This has made it possible to precisely monitor reforestation efforts, identify deforestation hotspots, and automatically classify different types of land cover [26]. The second stage is the analysis of changes in forest cover, which uses models to pinpoint and measure shifts over time in both forested and non-forested areas .

ISSN 2072-3857

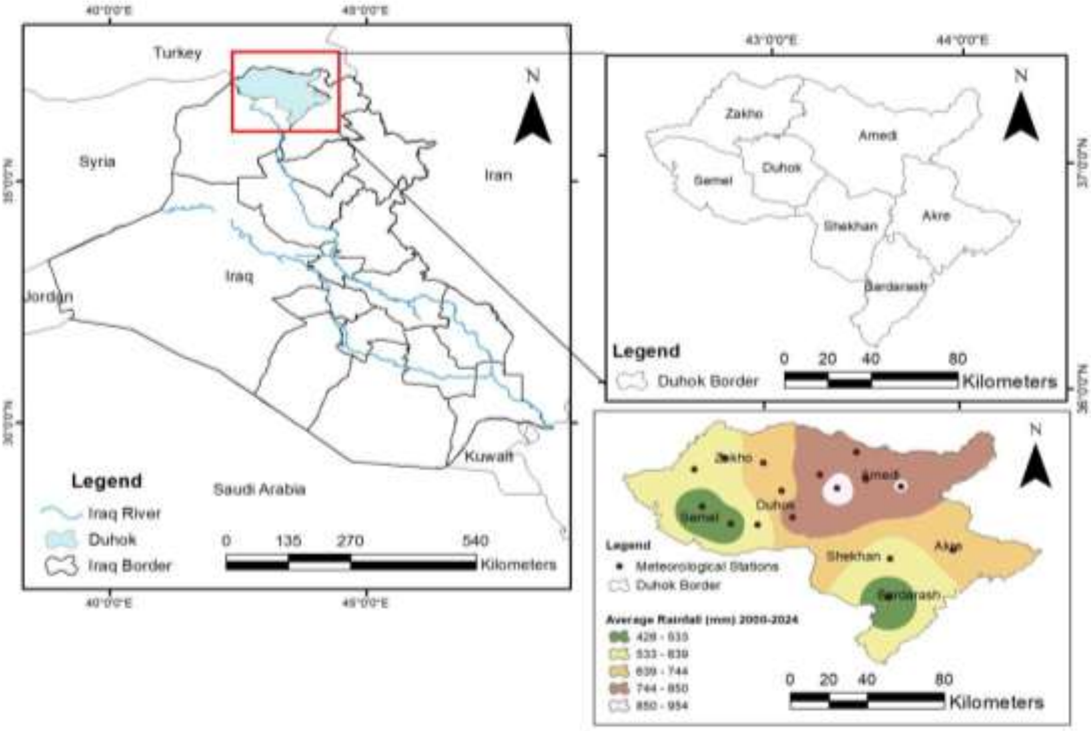

Figure 1 (A) Cartographic representation of Iraq, (B) Cartographic representation of the study area in the DU Government

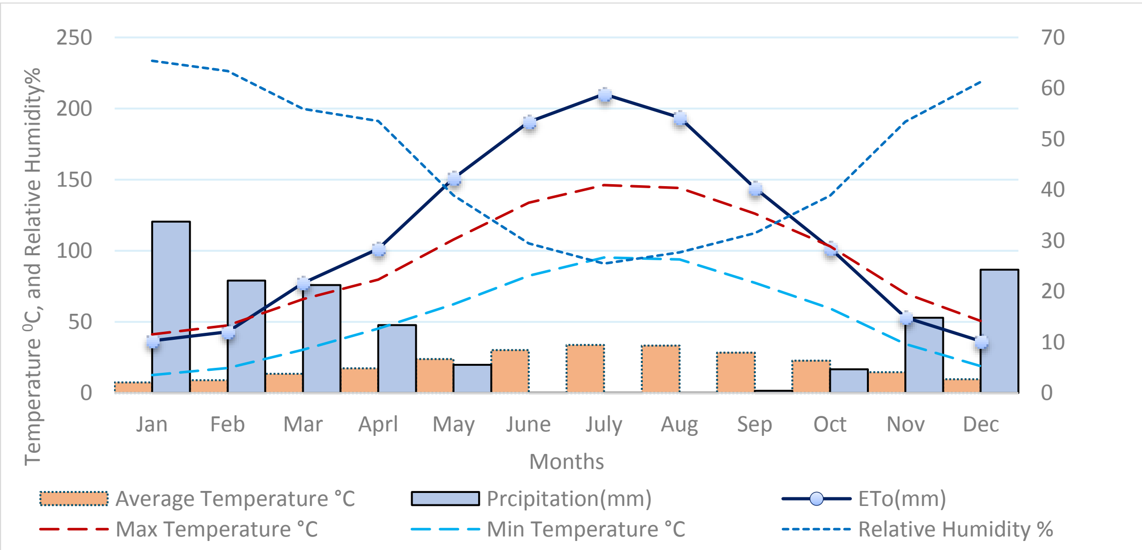

Figure 2 Monthly precipitation, relative humidity, actual evaporation, maximum, minimum, and mean temperature of DU Government for the period spanning from 1997 to 2023.

Satellite Image Data

Sentinel-2 Data

The June 2015-launched Sentinel-2A and Sentinel-2B satellites include Multi-Spectral Instruments (MSI) that can collect data across a 290-kilometer area every five days. These

ISSN 2072-3857

sensors cover 13 spectral bands, including three 60-meter atmospheric bands, six 20-meter red-edge, near-infrared, and shortwave infrared bands, and four 10-meter visible and near-infrared bands. Sentinel-2B MSI's Level-1C top-of-atmosphere reflectance data were used for this analysis. Four Sentinel-2A MSI images from 2017 to 2024 were retrieved from the ESA Copernicus Sentinels Scientific Data Hub and processed utilizing the Sen2Cor processor (v2.4.0) to derive Level-2A land surface reflectance, rectifying for atmospheric effects[27]. To assess temporal changes in Duhok Province from 2000 to 2024, a total of 48 Sentinel satellite images with a spatial resolution of 10 meters were utilized, comprising two images per year.

Landsat Datasets

For this study, we acquired Landsat images (OLI/TIRS C1 Level-1) and Landsat 7 ETM+ data from 2000 to 2017 from USGS's GloVis, selecting images with less than 10% cloud cover (Figure 3). Atmospheric correction was performed using the FLAASH algorithm in ENVI 5.3, and vegetation indices like NDVI, LST, NDMI, and MSAVI2 were calculated for each Landsat image[28.[

Spectral Indices

NDVI Normalized Difference Vegetation Index

The NDVI index is calculated based on the reflectance of the red (Red) and the Near-Infrared (NIR) bands of the Landsat images, using formula 3.6, as follows:

NDVI=(NIR-Red)/(NIR+Red) ……………….....1

Theoretically, NDVI values ranged between −1.0 and +1.0. However, the typical range of the NDVI index from vegetation and other earth surface materials is between approximately −0.1 (NIR less than Red) for no vegetated surfaces and as high as 0.9 for dense vegetative cover. NDVI values increase with increasing green biomass, positive seasonal changes, and favorable factors (e.g., abundant precipitation) [29], [30], [31], [32]. NDVI-based vegetation density can be classified into 3 classes based on NDVI values [31], [32]. The USGS remote sensing phenology states the following: "NDVI values range from +1.0 to -1.0. Areas of barren rock, sand, or snow usually show very low NDVI values (for example, 0.1 or less). Sparse vegetation, such as shrubs and grasslands or senescing crops, may result in moderate NDVI values (approximately 0.2 to 0.5). High NDVI values (approximately 0.6 to 0.9) correspond to dense vegetation such as that found in temperate and tropical forests or crops at their peak growth stage"[31], [33]. Table 1 Based on the USGS Remote sensing phenology of NDVI vegetation cover class (Nath and Acharjee, 2013; El-Gammal et al., 2014; Aquino et al., 2018). Table1. shows the vegetation classes and NDVI values.

Table1 Vegetation classes and NDVI values .

Class	NDVI Classification Value
Bare soil and/or water (no vegetation)	NDVI ≤ 0
Very Low NDVI	0 < NDVI ≤ 0.2
Low to Moderately Low NDVI	0.2 < NDVI ≤ 0.6
Moderately High to High NDVI	0.6 < NDVI ≤1

The Modified Soil-Adjusted Vegetation Index (MSAVI2(

The second vegetation index included in this study, MSAVI2, is a revision of the modified soil-adjusted vegetation index (MSAVI). Like the Soil-Adjusted Vegetation Index (SAVI), MSAVI2 corrects for areas with a high degree of exposed soil. This index is a refinement of SAVI that minimizes user error in setting the correction factor by more reliably and simply calculating a soil brightness correction factor [35]. The index also ranges from -1 to +1 and is calculated per-pixel according to the following formula [36.[

MSAVI2= (2ρNIR+1-√((2ρNIR+1)^2-8*(ρNIR-ρRED)))/2…….2

Where ρ is the reflectance in the near-infrared (NIR) or red (RED)band. By normalizing the contribution of background soil signal to the integrated spectral reflectance, MSAVI2 is a better indicator of the vegetation signal than the NDVI in land areas, such as much of our study area, where exposed soil can be a significant component of the observed surface.

Land Surface Temperature (LST(

The LST fraction images were produced using the Landsat thermal bands, which are bands 6 of the L5 TM, L7 ETM+, and bands 10–11 of L8 TIRS. Brightness temperature can be calculated using Planck’s law [37]. Using Top of the Atmosphere (TOA) radiances obtained from TIR sensors. Band 6 of TM/ETM+ and Band 10 of OLI images were utilized for retrieving the LST images [38]. Equations used for converting digital numbers into land surface temperature in Landsat 8 are presented as follows:

Conversion of DN Digital Number to At Satellite Brightness Temperature:

TB = K2 / ln((K1 /Lλ)+ 1)............3

Where:

K1 = Band-specific thermal conversion constant

)In watts/meter squared * ster * μm(

K2 = Band-specific thermal conversion constant (in kelvin(

Lλ is the spectral radiance at the sensor’s aperture, measured in watts/(meter squared * ster * μm.(

Calculation of the Land Surface Temperature in Kelvin

T = TB / [1 + (λ * TB / ρ) lnε] …………4

Where:

λ = wavelength of emitted radiance

ρ = h * c/σ (1.438 × 10−2m·K(

h = Planck’s constant (6.626 × 10−34 J·s(

σ = Boltzmann constant (1.38 × 10−23 J/K(

c = velocity of light (2.998 × 108 m/s(

ε = emissivity, which is given by the following: [39[

ε = 1.009 + 0.047 ln (NDVI(

Conversion from Kelvin to Celsius

Tc= T-273.15 5

T = land surface temperature in Kelvin

Tc = land surface temperature in Celsius [37].

The temperature transformation of the thermal infrared band into the value of ground temperature is done used the following equations for Landsat 5 and Landsat 7:

Convert DN to radiance = 0.05518*(i1) +1.2378 …. 6
Convert radiance to Kelvin = 1260.56/log ((666.09/i1) +1) .. …..7
Convert Kelvin to Celsius = i1-273.15 ………… 8

Whereas, i1 = the reflectance of the thermal infrared band. where L is value of radiance in thermal infrared; T is ground temperature (K); Q is digital record; K1 and K2 are calibration coefficients: K1=666.09 W/ (m2 ster mm) and K2=1282.71 K; Lmin=0.1238 W/(m2 ster mm); and Lmax=1.500 W/(m2 ster mm.(

Normalized Difference Moisture Index (NDMI(

The Normalized Difference Moisture Index (NDMI) standardizes the various moisture response bands across the near-infrared (NIR) and shortwave infrared (SWIR) spectra as per Equation (9). The linear relationship between the NIR/SWIR ratio and leaf relative water content was initially identified by [40]. They computed the NDMI utilizing the following formula:

NDMI = (NIR − SWIR) / (NIR + SWIR) ...…. 9

NIR corresponds to the Near-Infrared spectrum, and SWIR pertains to the Shortwave Infrared spectrum. Data for these spectral bands can be derived from remote sensing technologies, such as satellite imagery. The NDMI scale spans from -1 to 1, where values closer to 1 signify abundant moisture levels within vegetation, whereas values nearing -1 indicate a moisture deficiency. Typically, vegetation undergoing water scarcity exhibits diminished NDMI values in contrast to thriving vegetation.

ISSN 2072-3857

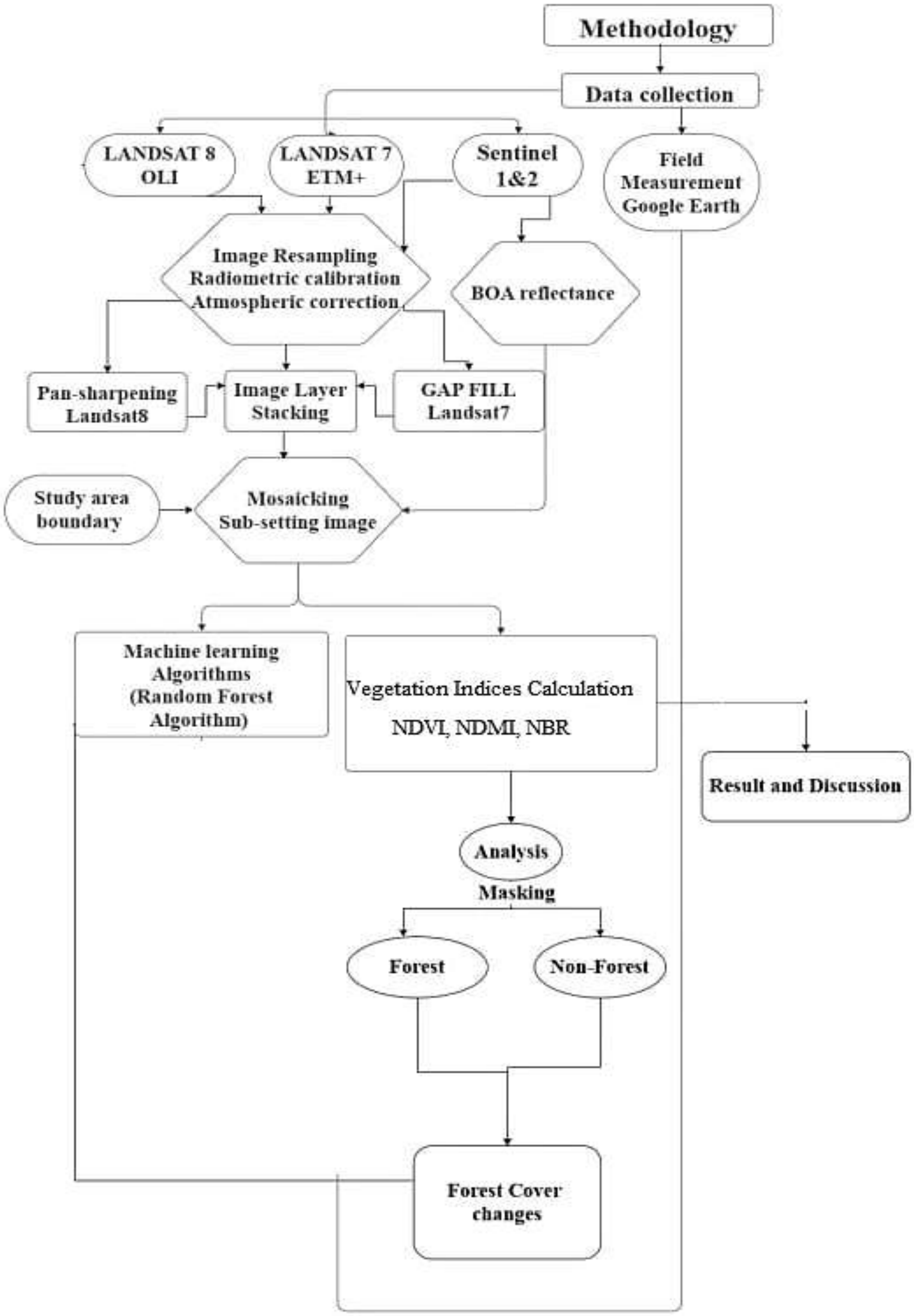

Figure 3 Flow diagram showing the methodology.

Results and Discussion

Forest Time Series Changes in Zakho District

The data presented in Table 2 reveals notable fluctuations in vegetation cover over time as indicated by the NDVI data. During the period from 2000 to 2001, approximately 716.6 km² (49.3%) of the terrain exhibited Forest Land coverage (NDVI). This coverage dropped to 521.8 km² (35.9%) by 2023–2024, indicating a significant decline in forests and land degradation. Widespread deforestation and conversion of forest land to other uses are shown by the growth in the area transitioning from Forest to Non-Forest (1 > 0) from 64.2 km² (4.4%) in 2000-2001 to 302.3 km² (20.8%) in subsequent years. In the meantime, there were a few Non-Forest to Forest (0 > 1) conversions, indicating little afforestation. Non-forest land (NDVI = 0) increased substantially from 639.9 km² (44%) in 2000 to 839.4 km² (57.8%) in 2023-2024, underscoring the expansion of barren and urbanized zones. These findings reveal an urgent need to curb forest land degradation and implement reforestation projects.

Table 2 Time series changes in NDVI for Zakho District from 2000 to 2024.

	Forest Land		Forest Land to Non-Forest Land		Non-Forest Land to Forest Land		Non-Forest Land	
Years	**Area (km²)**	**%**	**Area (km²)**	**%**	**Area (km²)**	**%**	**Area (km²)**	**%**
2000-2001	716.6	49.3	64.2	4.4	31.8	2.2	639.9	44.0
2001-2002	710.9	48.9	44.8	3.1	57.0	3.9	640.0	44.0
2002-2003	694.1	47.8	66.0	4.5	57.8	4.0	635.0	43.7
2003-2004	670.4	46.1	63.6	4.4	54.8	3.8	664.1	45.7
2004-2005	657.8	45.3	106.7	7.3	13.9	1.0	674.3	46.4
2005-2006	655.1	45.1	16.5	1.1	85.2	5.9	695.8	47.9
2006-2007	660.9	45.5	79.5	5.5	75.6	5.2	636.7	43.8
2007-2008	654.7	45.1	81.8	5.6	92.7	6.4	623.4	42.9
2008-2009	701.6	48.3	45.8	3.2	55.0	3.8	650.3	44.8
2009-2010	668.6	46.0	90.7	6.2	48.5	3.3	644.9	44.4
2010-2011	630.0	43.4	27.6	1.9	124.1	8.5	671.0	46.2
2011-	649.4	44.7	104.7	7.2	39.1	2.7	659.5	45.4

ISSN 2072-3857

2012								
2012-2013	613.6	42.2	74.9	5.2	71.7	4.9	692.5	47.7
2013-2014	648.2	44.6	37.0	2.5	48.8	3.4	718.7	49.5
2014-2015	629.4	43.3	67.6	4.7	44.8	3.1	710.9	48.9
2015-2016	622.9	42.9	51.2	3.5	70.9	4.9	707.7	48.7
2016-2017	581.1	40.0	112.1	7.7	73.9	5.1	684.4	47.1
2017-2018	597.0	41.1	58.5	4.0	54.8	3.8	742.4	51.1
2018-2019	596.7	41.1	55.1	3.8	56.1	3.9	744.8	51.3
2019-2020	568.0	39.1	84.8	5.8	23.5	1.6	776.4	53.4
2020-2021	547.5	37.7	44.0	3.0	87.8	6.0	773.4	53.2
2021-2022	553.2	38.1	82.1	5.7	49.2	3.4	768.1	52.9
2022-2023	542.0	37.3	60.5	4.2	40.2	2.8	810.0	55.7
2023-2024	521.8	35.9	60.4	4.2	31.1	2.1	839.4	57.8

Normalized Difference Moisture Index (NDMI) Time Series Change

The data illustrated in Table 3 reveals a discernible trend towards increased aridity in Zakho District over time. The NDMI analysis indicates the emergence of a Very Dry classification in recent years, marking the establishment of new regions characterized by severe moisture deficiency. The Dry category expanded from 340.9 km² (23.5%) in 2000 to 507.7 km² (34.9%) in 2023, illustrating an alarming increase in dry areas. Conversely, the Moderate Moisture zones decreased significantly, shrinking from 674.1 km² (46.4%) in 2000 to 421.8 km² (29%) in 2023, indicating reduced soil and vegetation moisture levels. Moist zones similarly declined, underscoring the shrinking extent of healthy vegetation. The Very Moist category initially covered 119.5 km² (8.2%) in 2000 but experienced a considerable reduction in subsequent years, indicating the gradual disappearance of wetlands and water-rich regions due to environmental stress. These NDMI trends emphasize the urgent need for water conservation, sustainable land management, and afforestation initiatives to mitigate the impact of declining moisture.

ISSN 2072-3857

Table 3 Time series changes in NDMI for Zakho District from 2000 to 2024.

	Very dry		Dry		Moderate		Moist		Very moist	
Years	Area (km^2)	%	Area (km^2)	%	Area (km^2)	%	Area (km^2)	%	Area (km^2)	%
2000-2001	0.0	0.0	340.9	23.5	674.1	46.4	318.3	21.9	119.5	8.2
2001-2002	0.0	0.0	483.8	33.3	624.2	43.0	253.0	17.4	91.8	6.3
2002-2003	0.0	0.0	382.3	26.3	628.7	43.3	331.4	22.8	110.3	7.6
2003-2004	0.0	0.0	380.4	26.2	780.4	53.7	211.6	14.6	80.3	5.5
2004-2005	0.0	0.0	383.4	26.4	693.3	47.7	285.5	19.7	90.5	6.2
2005-2006	5.3	0.4	464.9	32.0	618.4	42.6	282.1	19.4	82.0	5.6
2006-2007	11.5	0.8	502.7	34.6	725.7	49.9	161.9	11.1	50.8	3.5
2007-2008	166.1	11.4	585.1	40.3	435.6	30.0	197.3	13.6	68.7	4.7
2008-2009	318.5	21.9	608.9	41.9	293.2	20.2	173.2	11.9	59.4	4.1
2009-2010	200.2	13.8	610.4	42.0	372.1	25.6	184.8	12.7	85.2	5.9
2010-2011	205.4	14.1	569.5	39.2	408.7	28.1	201.3	13.9	67.8	4.7
2011-2012	0.8	0.1	223.7	15.4	753.8	51.9	333.7	23.0	140.6	9.7
2012-2013	356.3	24.5	600.9	41.4	318.7	21.9	142.9	9.8	33.8	2.3
2013-2014	325.3	22.4	518.8	35.7	301.2	20.7	206.3	14.2	101.1	7.0
2014-2015	336.0	23.1	498.6	34.3	361.2	24.9	181.3	12.5	75.5	5.2
2015-2016	218.7	15.1	505.9	34.8	403.2	27.7	235.8	16.2	89.1	6.1
2016-2017	215.1	14.8	465.3	32.0	444.4	30.6	229.2	15.8	98.7	6.8
2017-2018	84.9	5.8	440.5	30.3	568.6	39.1	283.5	19.5	75.2	5.2
2018-2019	304.4	21.0	564.4	38.8	346.9	23.9	170.8	11.8	66.2	4.6
2019-2020	84.6	5.8	402.7	27.7	566.6	39.0	284.8	19.6	114.0	7.8
2020-2021	220.1	15.1	463.6	31.9	470.7	32.4	220.0	15.1	78.3	5.4
2021-	236.7	16.3	544.3	37.5	416.5	28.7	196.3	13.5	58.8	4.0

ISSN 2072-3857

2022										
2022-2023	257.5	17.7	504.8	34.7	436.9	30.1	198.1	13.6	55.3	3.8
2023-2024	272.2	18.7	507.7	34.9	421.8	29.0	188.6	13.0	62.4	4.3

Modified Soil Adjusted Vegetation Index (MSAVI2) Time Series Change

The data depicted in Table 4 indicates a decline in stable vegetation cover. The MSAVI2 analysis reveals that Forest Land (MSAVI2) initially encompassed 595 km² (41%) in 2000 but diminished to 524.7 km²

(%36.1)by 2024, signifying a gradual deterioration in robust vegetation.The area transitioning from Forest to Non-Forest peaked at 302.3 km² (20.8%), further indicating extensive deforestation or land degradation. The Non-Forest to Forest transition remained minimal, covering only 18.2 km² (1.3%) in recent years, limited forest restoration. Conversely, Non-Forest Land expanded to 809.7 km² (55.7%) by 2024, representing a significant increase in barren areas. The analysis of LST, NDMI, NDVI, and MSAVI2 data for Zakho District reveals significant increases in surface temperatures, dryness, and non-forest land over time. Forest land has decreased substantially, indicating the detrimental impacts of deforestation, urbanization, and climate variability .

Table 4 Time series changes in MSAVI2 for Zakho District from 2000 to 2024 .

	Forest Land		Forest Land to Non-Forest Land		Non-Forest Land to Forest Land		Non-Forest Land	
Years	**Area (km²)**	**%**	**Area (km²)**	**%**	**Area (km²)**	**%**	**Area (km²)**	**%**
2000-2001	595.0	41.0	49.8	3.4	18.0	1.2	789.8	54.4
2001-2002	570.0	39.2	43.1	3.0	15.9	1.1	823.7	56.7
2002-2003	577.0	39.7	8.8	0.6	26.9	1.8	839.9	57.8
2003-2004	600.7	41.3	3.2	0.2	61.1	4.2	787.7	54.2
2004-2005	599.8	41.3	62.0	4.3	10.2	0.7	780.7	53.7
2005-2006	495.4	34.1	114.5	7.9	46.0	3.2	796.7	54.8
2006-2007	501.1	34.5	40.3	2.8	97.7	6.7	813.6	56.0
2007-2008	586.3	40.4	12.5	0.9	131.0	9.0	722.8	49.7
2008-2009	621.9	42.8	11.2	0.8	95.5	6.6	724.2	49.8
2009-2010	592.4	40.8	124.9	8.6	15.5	1.1	719.8	49.5
2010-2011	500.4	34.4	107.6	7.4	57.6	4.0	787.1	54.2
2011-2012	490.5	33.8	67.4	4.6	102.2	7.0	792.5	54.5
2012-2013	510.7	35.1	82.1	5.6	75.2	5.2	784.8	54.0
2013-2014	481.6	33.1	104.2	7.2	6.4	0.4	860.5	59.2
2014-2015	455.8	31.4	32.2	2.2	88.5	6.1	876.2	60.3
2015-2016	497.2	34.2	47.1	3.2	59.6	4.1	848.8	58.4
2016-2017	499.8	34.4	57.0	3.9	148.5	10.2	747.4	51.4
2017-2018	542.3	37.3	105.9	7.3	14.4	1.0	790.0	54.4

ISSN 2072-3857

2018-2019	546.7	37.6	10.0	0.7	243.1	16.7	652.8	44.9
2019-2020	540.1	37.2	249.8	17.2	6.6	0.5	656.2	45.2
2020-2021	536.2	36.9	10.5	0.7	278.2	19.1	627.8	43.2
2021-2022	512.2	35.2	302.3	20.8	8.0	0.6	630.3	43.4
2022-2023	496.8	34.2	23.4	1.6	23.4	1.6	886.3	61.0
2023-2024	524.7	36.1	18.2	1.3	100.0	6.9	809.7	55.7

Land Surface Temperature (LST) Time Series Change (2000–2024 (

The data illustrated in Table 5 reveals a significant transformation in the district's temperature distribution, as indicated by the analysis of variations in LST over time. In the year 2000, 218.4 square kilometers (15%) of the terrain was enveloped by Very Low LST (≤ 35°C). But by 2024, this coverage had drastically decreased to

17.8km² (1.2%), suggesting that urbanization and environmental change were to blame for the steep fall in colder zones. The decrease in chilly places is further highlighted by fluctuations during dry years. In 2000, the first coverage for the Low LST (35–40°C) category was 250.7 km² (17.3%). Although there was some fluctuation, this group continuously made up 16% to 20% of the whole region, suggesting that it has persisted despite more significant environmental changes. Rising surface temperatures were reflected in the Moderate LST (40–45°C) category, which at first spanned 460.2 km² (31.7%) in 2000 but then exhibited an increased trend, culminating at 754 km² (51.9%) in 2011. Similarly, the High LST (45-50°C) category expanded from 494.3 km² (34%) in 2000 to 848.1 km² (58.4%) in 2021, demonstrating intensified heat exposure and increased desertification .

ISSN 2072-3857

Table 5 Time series changes in LST for Zakho District from 2000 to 2024 .

	Very low ≤ 35		Low <35-40>		Moderate <40-45>		High <45-50>		Extreme ≥ 50	
Years	Area (km^2)	%	Area (km^2)	%	Area (km^2)	%	Area (km^2)	%	Area (km^2)	%
2000-2001	218.4	15.0	250.7	17.3	460.2	31.7	494.3	34.0	29.0	2.0
2001-2002	120.9	8.3	244.1	16.8	301.6	20.8	632.7	43.5	153.5	10.6
2002-2003	249.3	17.2	299.2	20.6	528.6	36.4	374.5	25.8	1.1	0.1
2003-2004	409.1	28.2	436.6	30.0	543.1	37.4	61.0	4.2	2.8	0.2
2004-2005	129.2	8.9	237.9	16.4	291.7	20.1	755.8	52.0	38.0	2.6
2005-2006	189.4	13.0	254.6	17.5	460.5	31.7	528.2	36.4	20.0	1.4
2006-2007	110.0	7.6	233.2	16.1	324.1	22.3	604.4	41.6	181.0	12.5
2007-2008	102.9	7.1	221.6	15.2	280.0	19.3	493.8	34.0	354.3	24.4
2008-2009	205.1	14.1	239.8	16.5	445.9	30.7	501.4	34.5	60.5	4.2
2009-2010	254.5	17.5	371.4	25.6	630.6	43.4	192.9	13.3	3.2	0.2
2010-2011	44.1	3.0	169.6	11.7	754.0	51.9	478.7	32.9	6.3	0.4
2011-2012	234.2	16.1	141.2	9.7	592.9	40.8	477.0	32.8	7.7	0.5
2012-2013	89.3	6.1	208.2	14.3	394.5	27.2	710.5	48.9	50.1	3.4
2013-2014	149.8	10.3	247.8	17.1	255.2	17.6	647.7	44.6	152.1	10.5
2014-2015	50.0	3.4	194.2	13.4	305.4	21.0	695.8	47.9	207.2	14.3
2015-2016	103.8	7.1	268.8	18.5	383.4	26.4	592.6	40.8	104.1	7.2
2016-2017	112.1	7.7	265.0	18.2	497.1	34.2	571.5	39.3	7.0	0.5
2017-2018	49.3	3.4	249.2	17.1	620.9	42.7	481.4	33.1	51.9	3.6
2018-2019	51.3	3.5	210.9	14.5	289.2	19.9	558.8	38.5	342.5	23.6
2019-2020	109.5	7.5	256.4	17.6	407.7	28.1	605.4	41.7	73.6	5.1
2020-2021	46.6	3.2	205.4	14.1	317.9	21.9	532.0	36.6	350.7	24.1
2021-	40.8	2.8	182.6	12.6	278.6	19.2	848.1	58.4	102.6	7.1

ISSN 2072-3857

2022										
2022-2023	24.4	1.7	147.5	10.2	531.1	36.5	604.1	41.6	145.6	10.0
2023-2024	73.7	5.1	293.4	20.2	676.9	46.6	404.4	27.8	4.3	0.3

The Extreme LST (≥ 50°C) category, covering 29 km² (2%) in 2000, peaked at 235.7 km² (16.2%) in 2024, indicating a considerable rise in heat-stressed zones due to reduced vegetation cover. These trends confirm a gradual shift toward hotter surface conditions, driven by deforestation, urban expansion, and climate stress.

Forest Time Series Changes in Duhok District Center

The data illustrated in Table 6 reveals that forested areas encompassed 622.8 km² (61.4%) in 2000, yet experienced a steady decline to 416.5 km² (41%) by 2024, indicating a substantial loss of forest cover. The transition from forested to non-forested areas (1 > 0) has escalated, signifying both land degradation and the conversion to urban and agricultural utilization. The non-forest to forest category remained minimal, indicating limited regrowth or afforestation efforts. The non-forested land expanded from 283.7 km² (28%) to 513.4 km² (50.6%) over the years, illustrating an increase in barren and urbanized areas.

Table 6 Time series changes in NDVI for Duhok District from 2000 to 2024.

	Forest Land		**Forest Land to Non-Forest Land**		**Non-Forest Land to Forest Land**		**Non-Forest Land**	
Years	**Area (km²)**	**%**	**Area (km²)**	**%**	**Area (km²)**	**%**	**Area (km²)**	**%**
2000-2001	622.8	61.4	69.0	6.8	38.7	3.8	283.7	28.0
2001-2002	589.2	58.1	72.3	7.1	32.6	3.2	320.2	31.5
2002-2003	551.2	54.3	70.9	7.0	136.3	13.4	255.9	25.2
2003-2004	589.4	58.1	98.1	9.7	53.8	5.3	273.0	26.9
2004-2005	545.0	53.7	97.7	9.6	22.5	2.2	349.1	34.4
2005-2006	551.9	54.4	15.5	1.5	82.9	8.2	364.0	35.9
2006-2007	537.8	53.0	97.0	9.6	59.4	5.9	320.1	31.5
2007-2008	528.5	52.1	68.7	6.8	103.4	10.2	313.7	30.9
2008-2009	512.5	50.5	119.5	11.8	35.1	3.5	347.2	34.2
2009-	469.1	46.2	78.5	7.7	103.8	10.2	362.9	35.

ISSN 2072-3857

2010								8
2010-2011	523.9	51.6	49.1	4.8	55.3	5.4	386.1	38.0
2011-2012	481.4	47.4	97.8	9.6	58.0	5.7	377.2	37.2
2012-2013	451.0	44.4	88.3	8.7	85.3	8.4	389.6	38.4
2013-2014	475.9	46.9	60.5	6.0	34.1	3.4	443.9	43.7
2014-2015	483.3	47.6	26.7	2.6	91.1	9.0	413.2	40.7
2015-2016	511.2	50.4	63.2	6.2	34.4	3.4	405.5	39.9
2016-2017	437.6	43.1	108.0	10.6	60.2	5.9	408.5	40.2
2017-2018	451.6	44.5	46.1	4.5	48.3	4.8	468.2	46.1
2018-2019	470.5	46.4	29.5	2.9	79.9	7.9	434.4	42.8
2019-2020	466.2	45.9	84.1	8.3	20.2	2.0	443.7	43.7
2020-2021	438.2	43.2	48.2	4.8	74.9	7.4	452.9	44.6
2021-2022	430.8	42.4	82.3	8.1	29.3	2.9	471.8	46.5
2022-2023	413.3	40.7	46.8	4.6	46.6	4.6	507.5	50.0
2023-2024	416.5	41.0	43.4	4.3	41.0	4.0	513.4	50.6

Normalized Difference Moisture Index (NDMI) Time Series Change in Duhok District Center

The data depicted in Table 7 reveals a notable trend in moisture content. The category of "Very Dry" was scarce in the earlier years but has sporadically emerged recently, indicating a growing moisture deficit. Conversely, the category of "Dry" has substantially expanded, from 233.7 km² (23%) in 2000 to 349.8 km² (34.5%) in 2024, signifying a significant increase in aridity. Conversely, moderate zones showed a gradual decrease, starting at 559.6 km² (55.1%) in 2000 and dropping to 428.4 km² (42.2%) in 2024. The moist category also declined, from 198 km² (19.5%) in 2000 to 194.9 km² (19.2%) in 2024, pointing to a reduction in healthy vegetation and water bodies. The "Very Moist" zones, covering 23 km² (2.3%) initially, fell to 10.8 km² (1%) by 2024, further emphasizing a reduction in moisture-rich areas due to increasing environmental stress.

ISSN 2072-3857

Table 7 Time series changes in NDMI for Duhok District from 2000 to 2024.

	Very dry		Dry		Moderate		Moist		Very moist	
Years	**Area (km²)**	**%**	**Area (km²)**	**%**	**Area (km²)**	**%**	**Area (km²)**	**%**	**Area (km²)**	**%**
2000-2001	0.0	0.0	233.7	23.0	559.6	55.1	198.0	19.5	23.0	2.3
2001-2002	0.0	0.0	274.2	27.0	502.3	49.5	209.7	20.7	28.2	2.8
2002-2003	0.0	0.0	277.9	27.4	487.1	48.0	220.0	21.7	29.3	2.9
2003-2004	0.0	0.0	287.0	28.3	585.1	57.6	119.4	11.8	22.8	2.2
2004-2005	0.0	0.0	286.1	28.2	510.2	50.3	189.2	18.6	28.9	2.8
2005-2006	0.0	0.0	317.4	31.3	474.0	46.7	188.4	18.6	34.5	3.4
2006-2007	11.5	1.1	331.6	32.7	591.6	58.3	69.0	6.8	10.6	1.0
2007-2008	107.3	10.6	372.0	36.7	387.2	38.1	125.5	12.4	22.3	2.2
2008-2009	189.6	18.7	489.6	48.2	260.9	25.7	60.7	6.0	13.5	1.3
2009-2010	69.9	6.9	399.7	39.4	438.2	43.2	97.3	9.6	9.2	0.9
2010-2011	126.5	12.5	373.9	36.8	375.2	37.0	115.9	11.4	22.9	2.3
2011-2012	0.1	0.0	128.3	12.6	573.7	56.5	279.4	27.5	32.7	3.2
2012-2013	268.1	26.4	474.5	46.7	225.2	22.2	40.2	4.0	6.3	0.6
2013-2014	169.5	16.7	411.2	40.5	303.1	29.9	110.6	10.9	19.9	2.0
2014-2015	267.1	26.3	398.8	39.3	245.9	24.2	82.1	8.1	20.6	2.0
2015-2016	123.9	12.2	351.8	34.7	369.6	36.4	143.6	14.2	25.5	2.5
2016-2017	153.9	15.2	341.6	33.7	334.3	32.9	150.3	14.8	34.2	3.4
2017-2018	50.4	5.0	321.3	31.7	440.0	43.4	175.4	17.3	27.2	2.7
2018-2019	193.5	19.1	436.4	43.0	287.7	28.3	79.6	7.8	17.1	1.7
2019-2020	41.2	4.1	241.8	23.8	447.1	44.0	241.9	23.8	42.3	4.2
2020-2021	123.5	12.2	351.2	34.6	369.8	36.4	140.9	13.9	28.9	2.8

ISSN 2072-3857

2021-2022	145.9	14.4	446.4	44.0	299.7	29.5	102.4	10.1	19.8	2.0
2022-2023	142.6	14.1	410.6	40.5	356.3	35.1	88.3	8.7	16.4	1.6
2023-2024	159.9	15.8	428.4	42.2	314.5	31.0	94.4	9.3	17.1	1.7

Modified Soil Adjusted Vegetation Index (MSAVI2) Time Series Change in Duhok District Center

The data presented in Table 8 illustrates that Forest land initially covered an area of 487.2 km² (48%), which subsequently decreased to 409.5 km² (40.3%) by the year 2024, indicating a decline in the extent of healthy vegetation coverage . The conversion of forest land to non-forest areas experienced a notable surge, reaching a peak of 178.2 km² (17.6%), highlighting a significant level of forest degradation. Non-forest to forest transition remained low, with a peak of 14.4 km² (1.4%), demonstrating insufficient restoration. Non-forest land expanded to 571.8 km² (56.3%) by 2024, reflecting widespread land degradation.

Table 8 Time series changes in MSAVI2 for Duhok District from 2000 to 2024.

	Forest Land		**Forest Land to Non-Forest Land**		**Non-Forest Land to Forest Land**		**Non-Forest Land**	
Years	**Area (km²)**	**%**	**Area (km²)**	**%**	**Area (km²)**	**%**	**Area (km²)**	**%**
2000-2001	487.2	48.0	45.0	4.4	43.0	4.2	439.1	43.3
2001-2002	434.0	42.8	96.2	9.5	7.7	0.8	476.5	46.9
2002-2003	425.0	41.9	16.7	1.6	31.1	3.1	541.6	53.4
2003-2004	451.3	44.5	4.8	0.5	68.8	6.8	489.5	48.2
2004-2005	475.3	46.8	44.7	4.4	23.6	2.3	470.7	46.4
2005-2006	398.8	39.3	100.1	9.9	50.6	5.0	464.8	45.8
2006-2007	386.8	38.1	62.6	6.2	106.2	10.5	458.7	45.2
2007-2008	407.3	40.1	85.8	8.4	70.4	6.9	450.9	44.4
2008-2009	383.1	37.7	54.4	5.4	94.6	9.3	482.3	47.5
2009-2010	436.9	43.0	40.7	4.0	97.1	9.6	439.6	43.3
2010-2011	355.8	35.1	178.2	17.6	50.3	5.0	430.1	42.4
2011-2012	305.9	30.1	100.2	9.9	109.1	10.8	499.1	49.2
2012-2013	332.8	32.8	82.2	8.1	92.0	9.1	507.3	50.0
2013-2014	278.9	27.5	146.0	14.4	5.6	0.5	583.9	57.5
2014-2015	276.7	27.3	7.7	0.8	170.3	16.8	559.5	55.1
2015-2016	389.7	38.4	57.4	5.7	29.3	2.9	537.9	53.0
2016-2017	359.9	35.5	59.1	5.8	134.6	13.3	460.7	45.4
2017-2018	392.5	38.7	102.0	10.1	10.1	1.0	509.6	50.2
2018-2019	398.6	39.3	4.0	0.4	279.5	27.5	332.1	32.7
2019-2020	440.6	43.4	237.5	23.4	2.5	0.2	333.7	32.9
2020-2021	435.4	42.9	7.7	0.8	245.2	24.2	326.0	32.1
2021-2022	372.3	36.7	308.3	30.4	7.2	0.7	326.5	32.2
2022-2023	358.9	35.4	20.7	2.0	62.9	6.2	571.8	56.3

ISSN 2072-3857

2023-2024	409.5	40.3	12.4	1.2	115.0	11.3	477.5	47.0

Land Surface Temperature (LST) Time Series Change (2000–2024) in Duhok District Center

The data illustrated in Table 9 reveals a noteworthy trend in the very low Land Surface Temperature (LST) category. Initially encompassing 12.3 km² (1.2%) in 2000, this category experienced a substantial decrease to a mere 1.7 km² (0.2%) by 2024. This decline signifies a significant reduction in areas with cooler temperatures, likely influenced by escalating urbanization and the impacts of climate change.The low LST category (35–40°C) also exhibited a downward trend, starting at 112.1 km² (11%) in 2000 and fluctuating across the years before settling at 9.9 km² (1%) in 2024. Meanwhile, the moderate LST category (40–45°C) represented a substantial portion of the district, covering 513.2 km² (50.6%) initially and fluctuating before rising to 489.6 km² (48.2%) by 2024. High LST zones (45–50°C) showed an upward trend, increasing from 359.8 km² (35.4%) in 2000 to 471.4 km² (46.5%) in 2024. The extreme LST category (≥ 50°C), though initially low at 16.9 km² (1.7%), expanded to 47.1 km² (4.6%) by 2024, underscoring the growing prevalence of heat-stressed areas. The data depicted in Figure 4 illustrates a substantial and consistent decline in forest land from 2000 to 2024, as evidenced by both the NDVI and MSAVI2 indices. According to the NDVI data, the coverage of forest land decreased from 44.1% (4861.3 km²) in the period of 2000–2006 to 36.2% (3989.1 km²) in the years 2018–2024, indicating an overall reduction of 8%. Similarly, the MSAVI2 index indicates a decline from 38.5% (4235.9 km²) to 35.1% (3870.2 km²), albeit suggesting a slight recovery in the timeframe of 2018–2024. This consistent pattern of forest loss underscores the persistent challenges of land degradation and deforestation throughout the study period. The conversion of forest land to non-forest land has increased over time. NDVI data show that forest-to-non-forest conversion rose from 2.2% (242.3 km²) in 2000–2006 to 2.9% (317.9 km²) in 2018–2024. MSAVI2 data reflects a more pronounced shift, with conversion rising from 2.3% (254.1 km²) to 4.3% (469.2 km²) in the same period. This suggests that MSAVI2 may be more sensitive to detecting small-scale forest degradation, capturing more nuanced changes than NDVI. Conversely, non-forest land recovery, indicating reforestation, has been minimal. NDVI data shows a near-constant rate of non-forest to forest conversion, remaining around 2.1% over the study period. In contrast, MSAVI2 data present a more optimistic view, with recovery increasing from 1.6% (180 km²) in 2000–2006 to 4.9% (538.1 km²) by 2018–2024. However, this recovery still does not offset the net forest loss observed in both indices.

ISSN 2072-3857

Table 9 Time series changes in LST for Duhok District from 2000 to 2024.

	Very low ≤ 35		Low <35-40>		Moderate <40-45>		High <45-50>		Extreme ≥ 50	
Years	**Area (km²)**	**%**	**Area (km²)**	**%**	**Area (km²)**	**%**	**Area (km²)**	**%**	**Area (km²)**	**%**
2000-2001	12.3	1.2	112.1	11.0	513.2	50.6	359.8	35.4	16.9	1.7
2001-2002	4.7	0.5	65.1	6.4	350.2	34.5	551.1	54.3	43.3	4.3
2002-2003	22.3	2.2	162.4	16.0	544.6	53.7	284.3	28.0	0.8	0.1
2003-2004	143.8	14.2	368.8	36.3	472.7	46.6	29.1	2.9	0.0	0.0
2004-2005	8.2	0.8	73.4	7.2	311.7	30.7	615.5	60.6	5.5	0.5
2005-2006	22.2	2.2	102.3	10.1	386.2	38.0	464.5	45.8	39.1	3.9
2006-2007	7.6	0.7	77.1	7.6	336.8	33.2	567.2	55.9	25.5	2.5
2007-2008	5.7	0.6	51.7	5.1	257.2	25.3	590.5	58.2	109.2	10.8
2008-2009	13.5	1.3	77.3	7.6	290.0	28.6	599.8	59.1	33.7	3.3
2009-2010	30.8	3.0	289.5	28.5	623.4	61.4	70.0	6.9	0.6	0.1
2010-2011	4.0	0.4	52.9	5.2	534.6	52.7	419.2	41.3	3.7	0.4
2011-2012	29.6	2.9	63.7	6.3	622.8	61.4	297.7	29.3	0.4	0.0
2012-2013	3.4	0.3	28.6	2.8	304.1	30.0	638.3	62.9	40.0	3.9
2013-2014	15.5	1.5	102.7	10.1	466.2	45.9	425.3	41.9	4.5	0.4
2014-2015	4.5	0.4	15.1	1.5	143.1	14.1	573.4	56.5	278.2	27.4
2015-2016	19.2	1.9	133.0	13.1	500.9	49.4	352.1	34.7	9.1	0.9
2016-2017	13.8	1.4	123.4	12.2	567.9	56.0	309.0	30.4	0.3	0.0
2017-2018	1.9	0.2	31.6	3.1	426.6	42.0	550.8	54.3	3.3	0.3
2018-2019	2.7	0.3	39.9	3.9	228.3	22.5	614.0	60.5	129.4	12.7
2019-2020	9.2	0.9	99.9	9.8	369.8	36.4	459.3	45.2	76.1	7.5
2020-2021	2.1	0.2	23.6	2.3	196.5	19.4	564.4	55.6	227.7	22.4
2021-	1.7	0.2	24.7	2.4	217.3	21.4	751.0	74.0	19.7	1.9

2022										
2022-2023	0.8	0.1	2.9	0.3	121.0	11.9	656.9	64.7	232.7	22.9
2023-2024	1.1	0.1	42.7	4.2	394.1	38.8	573.4	56.5	3.0	0.3

Deforestation trends are closely linked to changes in land surface temperatures. As forest coverage declined, the areas categorized as "Extreme" LST zones (≥ 50°C) slightly increased from 5.3% (583.4 km²) in 2000–2006 to 5.1% (565.5 km²) in 2018–2024. Additionally, the "High" LST zones (45–50°C) consistently occupied over 15% of the land area, indicating that areas with reduced vegetation cover experience higher surface temperatures. This reflects the direct environmental impact of deforestation, where the loss of vegetation leads to an increase in heat-stressed zones and exacerbates warming trends. The data illustrated in Figure 5 delineates the trends observed between the years 2000 and 2024 about regions with diminished vegetation moisture (NDMI) and elevated land surface temperatures (LST) within the Zakho and Duhok districts. Both localities demonstrate a substantial and persistent increase in areas characterized by environmental stress indicators

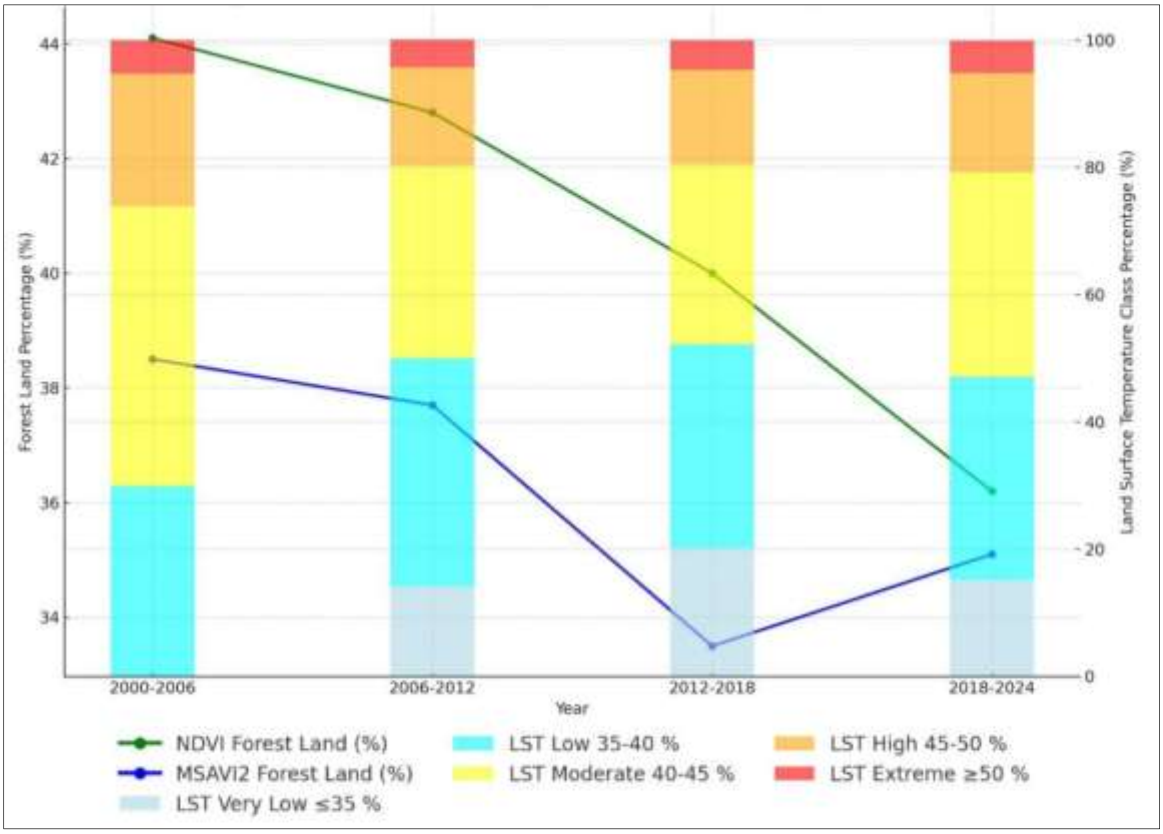

Figure 4 Integrated forest percentage and LST class percentage over time.

ISSN 2072-3857

Regarding low vegetation moisture, indicated by NDMI values, both Zakho and Duhok have seen a consistent upward trend, suggesting an increase in vegetation stress due to reduced moisture availability. Duhok district displays consistently larger areas affected by low NDMI, emphasizing a higher degree of moisture deficiency compared to Zakho. This suggests that Duhok might be more vulnerable to drought conditions, potentially exacerbating agricultural and ecological stress in the region. Simultaneously, the areas characterized by high land surface temperatures have notably increased in both Zakho and Duhok. Similar to the NDMI trend, Duhok district experiences larger areas with high LST, reflecting greater susceptibility to warming. This rise in land surface temperatures likely contributes to worsening drought conditions, accelerating vegetation degradation, and potentially increasing urban heat island effects. The simultaneous upward trends in both low NDMI and high LST strongly suggest interlinked environmental pressures. Rising temperatures likely reduce soil and vegetation moisture, further intensifying drought stress and negatively impacting vegetation health and land productivity. Such interlinked stresses indicate that both districts are experiencing significant environmental degradation and climate-driven challenges, calling for integrated and proactive management approaches. Given these findings, targeted mitigation strategies are essential .

Efforts should focus on promoting sustainable agricultural practices, reforestation, better water resource management, and urban planning strategies designed to alleviate heat stress and moisture loss. Such interventions are particularly critical for the Duhok district due to its greater vulnerability, indicated by larger affected areas

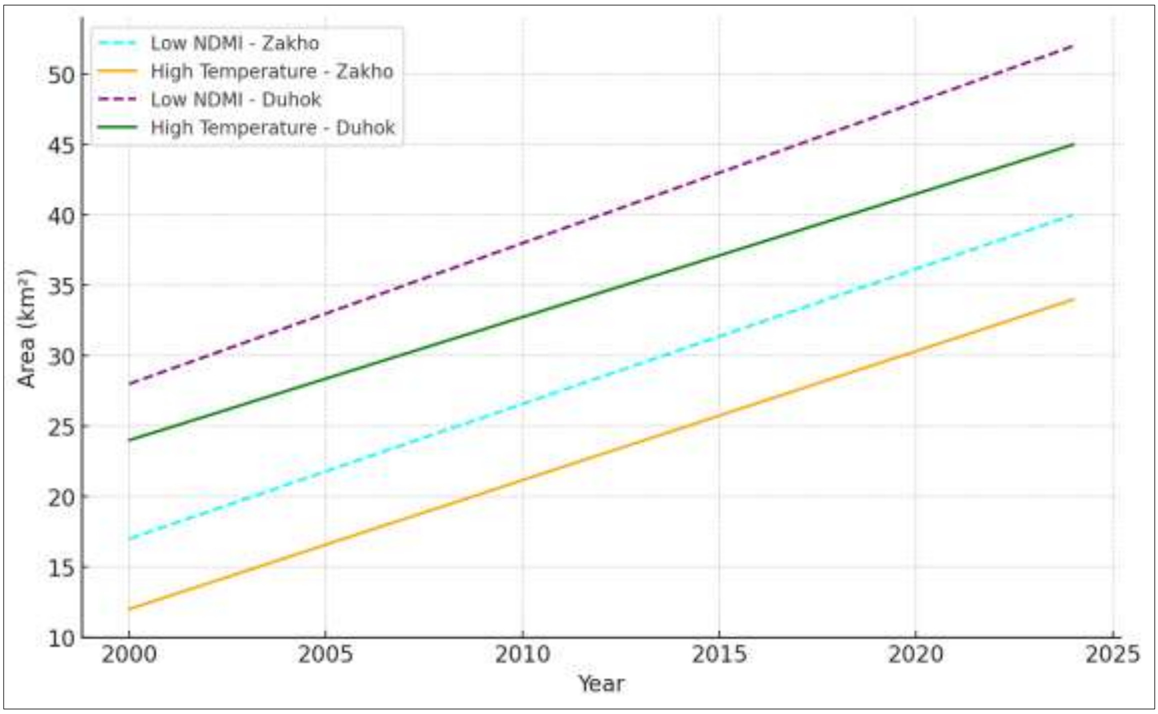

Figure 5 Comparison of low NDMI area and rising temperature area (2000-2024.(

ISSN 2072-3857

aConclusion

The results of this study highlight a consistent and alarming trend of environmental degradation across the Zakho and Duhok Districts. From 2000 to 2024, forest land has declined markedly, as reflected in NDVI and MSAVI2 indices, with conversion to non-forest areas intensifying due to urbanization, agricultural expansion, and climate stress. Moisture levels, as shown by NDMI, have dropped significantly, signaling worsening drought conditions and diminished vegetative health .

Concurrently, Land Surface Temperature (LST) data confirm increasing exposure to extreme heat, further exacerbating the impacts of deforestation and land degradation. Although some signs of vegetation recovery were detected, particularly in MSAVI2 data, these gains remain insufficient to reverse the overarching trend of forest loss. The linkage between forest decline and rising surface temperatures underscores the critical ecological consequences of continued environmental mismanagement and climate variability in the region.

The analysis highlights a critical trend of environmental degradation characterized by widespread deforestation, increased land aridity, and elevated surface temperatures .

In Zakho and Duhok, forested areas have contracted notably, transitioning into non-forest or degraded lands, as evidenced by shifts in NDVI and MSAVI2 data .

The NDMI findings further emphasize increasing dryness and a loss of moisture-rich zones, pointing to heightened vulnerability of soils and vegetation to drought stress. Meanwhile, the Duhok District Center exhibits a similar decline in forest health, with a corresponding expansion of barren land and urban areas .

Rising land surface temperatures (LST) confirm that once cooler zones have rapidly decreased, and extreme heat categories are becoming more prevalent, contributing to unfavorable conditions for both natural ecosystems and human activities.

Generally, the combined evidence of deforestation, diminishing moisture availability, and hotter surface temperatures underscores the severity of anthropogenic impacts, climate variability, and unsustainable land-use practices. Without immediate and coordinated remedial measures, these districts risk further ecological decline, adversely affecting biodiversity, water resources, and local livelihoods.

Recommendations

Initiate comprehensive reforestation and afforestation programs prioritizing native species to rehabilitate degraded lands and enhance biodiversity.

Enforce robust legislation and monitoring mechanisms to control illegal logging and unsustainable urban and agricultural expansion.

Promote sustainable water management practices, including rainwater harvesting, watershed protection, and irrigation efficiency.

Implement urban planning strategies incorporating green spaces to reduce surface temperature and improve microclimatic conditions.

Strengthen continuous environmental monitoring and research efforts using remote sensing indices to inform policy and management strategies effectively.

Foster community engagement and awareness programs emphasizing conservation and sustainable environmental practices to facilitate effective local stewardship of natural resources.

Author Contributions :

Conceptualization, N.M.A, M. H. and H.A.A.G.; Data curation, N.M.A, M. H. And H.A.A.G.; Formal analysis, N.M.A, M. H. and H.A.A.G.; Inves- tigation, N.M.A, M. H. and H.A.A.G.; Methodology, N.M.A, M. H. and H.A.A.G.; Resources, N.M.A and.; Supervision, M. H. and H.A.A.G.; Validation, N.M.A.; Visualization, N.M.A, M. H. and H.A.A.G.; Writing—original draft, N.M.A.; Writing—review and editing, M. H. and H.A.A.G. All authors have read and agreed to the published version of the manuscript.

Funding: This study has received partial funding from College of Agricultural Engineering Sciences, University of Duhok, Kurdistan Region, Iraq.

.

Data Availability Statement: Some data in this manuscript were obtained from the Ministry of Agriculture and Water Resources, Kurdistan Region, Iraq, while other data was provided by the United States Geological Service (USGS), along with Landsat images, and Sentinel being freely available on its website and statistical analysis of the parameters.

Acknowledgements: The authors would like to thank the United States Geological Service (USGS) for providing the Landsat images freely on its website. We are extremely grateful to the anonymous reviewers for their insightful comments and suggestions that significantly enhanced the quality of our paper.; the Ministry of Agriculture and Water Resources, Water Resources Department, Department of Forestry, and College of Agricultural Engineering Sciences, University of Duhok-Duhok and Salahaddin University-Erbil, Kurdistan Region, Iraq, for their valuable support.

Conflicts of Interest: The authors declare no conflict of interest

References

[1] K. G. Austin et al., "The economic costs of planting, preserving, and managing the world's forests to mitigate climate change," Nat. Commun., vol. 11, no. 1, p. 5946, 2020.

[2] R. M. Fokeng, W. G. Forje, V. M. Meli, and B. N. Bodzemo, "Multi-temporal forest cover change detection in the Metchie-Ngoum protection forest reserve, West Region of Cameroon," Egypt. J. Remote Sens. Sp. Sci., vol. 23, no. 1, pp. 113–124, 2020.

[3] R. Sekizawa, K. Ichii, and M. Kondo, "Satellite-based detection of evacuation-induced land cover changes following the Fukushima Daiichi nuclear disaster," Remote Sens. Lett., vol. 6, no. 11, pp. 824–833, 2015.

[4] V. Butsic, M. Baumann, A. Shortland, S. Walker, and T. Kuemmerle, "Conservation and conflict in the Democratic Republic of Congo: The impacts of warfare, mining, and protected areas on deforestation," Biol. Conserv., vol. 191, pp. 266–273, 2015.

[5] V. Butsic, M. Baumann, A. Shortland, S. Walker, and T. Kuemmerle, "Conservation and conflict in the Democratic Republic of Congo: The impacts of warfare, mining, and protected areas on deforestation," Biol. Conserv., vol. 191, pp. 266–273, 2015, doi: 10.1016/j.biocon.2015.06.037.

[6] L. Eklund, A. Persson, and P. Pilesjö, "Cropland changes in times of conflict, reconstruction, and economic development in Iraqi Kurdistan," Ambio, vol. 45, pp. 78–88, 2016.
[7] R. Burgess, E. Miguel, and C. Stanton, "War and deforestation in Sierra Leone," Environ. Res. Lett., vol. 10, no. 9, 2015, doi: 10.1088/1748-9326/10/9/095014.
[8] P. Dinc, L. Eklund, A. Shahpurwala, A. Mansourian, A. Aturinde, and P. Pilesjö, "Fighting insurgency, ruining the environment: The case of forest fires in the Dersim province of Turkey," Hum. Ecol., vol. 49, no. 4, pp. 481–493, 2021.
[9] W. Xu, X. Jin, J. Liu, X. Yang, J. Ren, and Y. Zhou, "Analysis of spatio-temporal changes in forest biomass in China," J. For. Res., vol. 33, no. 1, pp. 261–278, 2022.
[10] F. D. W. Witmer, "Remote sensing of violent conflict: eyes from above," Int. J. Remote Sens., vol. 36, no. 9, pp. 2326–2352, 2015.
[11] H. D. Venema, P. H. Calamai, and P. Fieguth, "Forest structure optimization using evolutionary programming and landscape ecology metrics," Eur. J. Oper. Res., vol. 164, no. 2, pp. 423–439, 2005.
[12] V. Gorsevski, E. Kasischke, J. Dempewolf, T. Loboda, and F. Grossmann, "Analysis of the Impacts of armed conflict on the Eastern Afromontane forest region on the South Sudan—Uganda border using multitemporal Landsat imagery," Remote Sens. Environ., vol. 118, pp. 10–20, 2012.
[13] S. Singh, A. Bhardwaj, and V. K. Verma, "Remote sensing and GIS based analysis of temporal land use/land cover and water quality changes in Harike wetland ecosystem, Punjab, India," J. Environ. Manage., vol. 262, p. 110355, 2020.
[14] L. Liu, Q. Niu, J. Heng, H. Li, and Z. Xu, "Transition characteristics of the dry-wet regime and vegetation dynamic responses over the Yarlung Zangbo River Basin, Southeast Qinghai-Tibet Plateau," Remote Sens., vol. 11, no. 10, p. 1254, 2019.
[15] C. Xu et al., "Runoff and soil erosion responses to rainfall and vegetation cover under various afforestation management regimes in subtropical montane forest," L. Degrad. Dev., vol. 30, no. 14, pp. 1711–1724, 2019.
[16] E. L. Boogaard, "Remote sensing assessment of the impact of the 2018 and 2019 droughts on the forests in The Netherlands," 2021, University of Twente.
[17] D. Delgado-Moreno and Y. Gao, "Forest degradation estimation through trend analysis of annual time series NDVI, NDMI and NDFI (2010–2020) using landsat images," in International Conference on Geospatial Information Sciences, Springer, 2021, pp. 149–159.
[18] M. Hossain and S. Wong, "Remote Sensing and GIS Application to Mangrove Forest Mapping in the Meghna Deltaic Islands of Bangladesh," Bangladesh J. …, vol. 1, no. April 2016, pp. 81–96, 2009, [Online]. Available: http://scholar.google.com
[19] Y. T. Mustafa and M. J. Noori, "Satellite remote sensing and geographic information systems (GIS) to assess changes in the water level in the Duhok dam," Int. J. Water Resour. Environ. Eng., vol. 5, no. 6, pp. 351–359, 2013, doi: 10.5897/IJWREE2012.0402.
[20] L. Eklund, "Migration Patterns in Duhok Governorate, Iraq, 2000-2010," Open Geogr. J., vol. 5, no. 1, pp. 48–58, 2012, doi: 10.2174/1874923201205010048.

[21] U. Nations, “G LOBAL F OREST R ESOURCES A SSESSMENT 2010 C OUNTRY R EPORT,” 2010.

[22] Resources, “Review of the Agricultural Sector In The Kurdistan Region Of Iraq: Analysis On Crops, Water Resources And Irrigation, And Selected Value Chains,” Annu. Rport, 2019.

[23] D. P. Roy et al., “Landsat-8: Science and product vision for terrestrial global change research,” Remote Sens. Environ., vol. 145, pp. 154–172, 2014.

[24] U. M. Bohlmann and V. F. Koller, “ESA and the Arctic-The European Space Agency’s contributions to a sustainable Arctic,” Acta Astronaut., vol. 176, pp. 33–39, 2020.

[25] F. Niro et al., “European Space Agency (ESA) calibration/validation strategy for optical land-imaging satellites and pathway towards interoperability,” Remote Sens., vol. 13, no. 15, p. 3003, 2021.

[26] M. Belgiu and L. Drăguţ, “Random forest in remote sensing: A review of applications and future directions,” ISPRS J. Photogramm. Remote Sens., vol. 114, pp. 24–31, 2016.

[27] C. Isbaex and A. M. Coelho, The potential of Sentinel-2 satellite images for land-cover/land-use and forest biomass estimation: A review. IntechOpen, 2021.

[28] SUHET, “EL-2 User Handbook Sentinel-2 User Handbook,” Ind. Eng. Chem., vol. 48, no. 9, pp. 1404–1406, 2015, doi: 10.1021/ie51400a018.

[29] A. Anyamba and C. J. Tucker, “Historical perspectives on AVHRR NDVI and vegetation drought monitoring,” Remote Sens. Drought Innov. Monit. Approaches, pp. 23–49, 2012, doi: 10.1201/b11863.

[30] C. Schmidt, “Remote Sensing of Drought,” Natl. Aeronaut. Sp. Adm. Appl. Remote Sens. Train. http//arset.gsfc.nasa.gov, 2017, [Online]. Available: http://ezproxy.utwente.nl:2218/doi/book/10.1201/b11863

[31] D. do N. Aquino, O. C. da R. Neto, M. A. Moreira, A. dos S. Teixeira, and E. M. de Andrade, “Use of remote sensing to identify areas at risk of degradation in the semi-arid region,” Rev. Cienc. Agron., vol. 49, no. 3, pp. 420–429, 2018, doi: 10.5935/1806-6690.20180047.

[32] A. Taufik, S. S. S. Ahmad, and N. F. E. Khairuddin, “Classification of Landsat 8 Satellite Data using Fuzzy c-means,” Proc. 2017 Int. Conf. Mach. Learn. Soft Comput. - ICMLSC ’17, no. January 2016, pp. 58–62, 2017, doi: 10.1145/3036290.3036330.

[33] B. Nath and S. Acharjee, “Forest Cover Change Detection using Normalized Difference Vegetation Index (NDVI) : A Study of Reingkhyongkine Lake ’ s Adjoining Areas ,” Indian Cartogr., vol. XXXIII, no. 2, pp. 348–403, 2013.

[34] M. I. El-Gammal, R. R. Ali, and R. M. Abou Samra, “NDVI Threshold Classification for Detecting Vegetation Cover in Damietta Governorate, Egypt,” J. Am. Sci., vol. 10, no. 8, pp. 108–113, 2014, doi: 10.1088/1361-6560/aad43f.

[35] J. Qi, Y. Kerr, and A. Chehbouni, “External factor consideration in vegetation index development,” Proc. 6th Int. Symp. Phys. Meas. Signatures Remote Sensing, ISPRS, no. February, pp. 723–730, 1994, doi: 95N17071.

[36] J. Qi, Y. Kerr, and A. Chehbouni, “External factor consideration in vegetation index development,” Proc. Phys. Meas. Signatures Remote Sens., no. August 2015, pp. 723–730, 1994, [Online]. Available: https://www.researchgate.net/publication/2362

1794_External_factor_consideration_in_vegetation_index_development
[37] P. Dash, F. M. Göttsche, F. S. Olesen, and H. Fischer, “Land surface temperature and emissivity estimation from passive sensor data: Theory and practice-current trends,” Int. J. Remote Sens., vol. 23, no. 13, pp. 2563–2594, 2002, doi: 10.1080/01431160110115041.
[38] Q. Sun, J. Tan, and Y. Xu, “An ERDAS image processing method for retrieving LST and describing urban heat evolution: A case study in the Pearl River Delta Region in South China,” Environ. Earth Sci., vol. 59, no. 5, pp. 1047–1055, 2009, doi: 10.1007/s12665-009-0096-3.
[39] and M. K. Donglian Sun, “Note on the NDVI-LST relationship and the use of temperature-related drought indices over North America,” Geophys. Res. Lett., vol. 34, no. 24, pp. 1–4, 2007, doi: 10.1029/2007GL031485.
[40] E. R. Hunt and B. N. Rock, “Detection of changes in leaf water content using Near- and Middle-Infrared reflectances,” Remote Sens. Environ., vol. 30, no. 1, pp. 43–54, 1989, doi: 10.1016/0034-4257(89)90046-1.